Materials Chemistry and Physics 137 (2013) 910–915

Contents lists available at SciVerse ScienceDirect

Materials Chemistry and Physics

journal homepage: www.elsevier.com/locate/matchemphys

Mechanical properties of epoxy composites reinforced with a low volume fraction of nanosilica fillers

M. Conradi [a,*], M. Zorko [b], A. Kocijan [a], I. Verpoest [c]

[a] Institute of Metals and Technology, Lepi Pot 11, 1000 Ljubljana, Slovenia
[b] National Institute of Chemistry, Hajdrihova 19, 1000 Ljubljana, Slovenia
[c] Department of Metallurgy and Materials, K. U. Leuven, Kasteelpark Arenberg 44, 3001 Heverlee, Belgium

HIGHLIGHTS

- Optimization of low volume fraction nanosilica/epoxy composite preparation.
- 10–20% increase of modulus of elasticity of 30 nm and 130 nm silica/epoxy composite.
- 25–30% improved toughening of 30 nm and 130 nm silica/epoxy composite.
- Increased resistance to failure silica size dependant.
- The crack propagating in the matrix avoiding the particles.

ARTICLE INFO

Article history:
Received 30 July 2012
Received in revised form
8 October 2012
Accepted 1 November 2012

Keywords:
Composite materials
Polymers
Elastic properties
Fracture
Impact test

ABSTRACT

In this paper we focus on the preparation and mechanical properties of the nanosilica-reinforced, epoxy resin Epikote 828LVEL. Epoxy composites containing two sizes of spherical silica nanoparticles, 130 nm and 30 nm, were prepared at a fixed volume fraction (V_P = 0.5%). To prevent agglomeration, the silica fillers were initially pre-treated with diglycidyl ether of bisphenol A (BADGE). Due to the low content of silica fillers, their inclusion in the matrix was confirmed by the increased roughness of a fracture surface compared to the smooth surface of the neat epoxy. Raman spectroscopy was employed to obtain additional information about the crack-propagation path. The mechanical properties, characterized by a three-point bending test, revealed a 10–20% increase in the composite's modulus of elasticity with 30-nm and 130-nm silica-filler inclusions. Elongation at break, on the other hand, decreased for 5–10% in both composites compared to neat epoxy, suggesting brittle fracture behavior in silica/epoxy composites. The fracture toughness results showed a 25–30% improved toughening for both composites compared to the pure epoxy. The composite's resistance to failure in terms of the impact energy was, however, strongly dependent on the size of the silica: we observed a 30% increase for the 130-nm, and a 60% increase for the 30-nm, silica/epoxy composites, compared to the pure epoxy.

1. Introduction

Epoxy resin is an engineering material used in many industrial products because of its good mechanical characteristics, such as a high modulus, excellent adhesion strength and low creep [1]. However, as pure epoxy is normally rather brittle, due to its highly cross-linked structure, a lot of attention has been paid to improving its mechanical properties by reinforcing the resin with various fillers, the improvement being due to the effects of the particle volume fraction, size, surface characteristics and the degree of particle dispersion [2–5]. Reinforcement agents such as glass particles [5,6], ceramic particles [7], layered silicates [8–10], metal particles [11], rubber plastics [12] and thermoplastics [13,14] have already been successfully employed.

Several researchers have studied the effects of particle size and volume fraction on the mechanical response of polymer composites [5,15–19]. There are a few analytical models based on crack propagation along the particle surfaces, taking the interspacing between the particles into account [20], as well as mathematically considered trapping, pinning and bridging of the crack front at the particles [21–23]. It has been shown that the fracture phenomena in composites filled with nanometer-sized particles is different to the behavior of composites filled with micrometer-sized or larger filler particles.

* Corresponding author. Tel.: +386 1 4701 972; fax: +386 1 4701 939.
E-mail address: marjetka.conradi@imt.si (M. Conradi).

0254-0584/$ – see front matter © 2012 Elsevier B.V. All rights reserved.
http://dx.doi.org/10.1016/j.matchemphys.2012.11.001

Silica/epoxy composites are one of the most widely used structural materials in the electronics, automotive and aerospace industries due to their ability to sustain mechanical as well as thermal loading [24]. Most of the research on silica/epoxy composites has concentrated on studying the effects of particle size and volume fraction, mostly high particle loadings (i.e., $V_F > 10\%$), on the mechanical properties [6,19,25]. Not a lot of attention has been paid to studying the mechanical response of silica/epoxy composites in the limit of a low volume fraction of silica fillers.

In this research the effects of particle size on the elastic modulus, the fracture toughness and the resistance to failure of epoxy composites filled with 0.5% volume fractions of 130-nm and 30-nm silica particles were investigated. To prevent agglomeration the silica particles were pre-treated with the bisphenol-A-type surfactant, which is compatible with the Epikote 828LVEL epoxy resin. The fracture surfaces of the specimens were observed with a scanning electron microscope (SEM) to distinguish between the neat epoxy and the epoxy composite after the addition of the silica particles. The crack-propagation path was additionally analyzed with Raman spectroscopy. The mechanical properties of the specimens were then characterized with a three-point bending test, a fracture-toughness test and the Charpy impact-strength test.

2. Experimental

2.1. Materials

The epoxy resin (Epikote 828LVEL, Momentive Specialty Chemicals B.V.) was mixed with the hardener 1,2-Diaminocyclohexane (Dytek DCH-99, Invista Nederland B.V.) in proportions of 100:15.2 wt.% and used as the matrix in the composite. Silica (SiO_2) nanoparticles with diameters of 30 nm and 130 nm were used as the reinforcement. The 30-nm silica nanospheres were provided by Riedel-de Haën (Silica Cab-osil), while the 130-nm silica particles were synthesized following the Stöber–Fink–Bohn method [26]. Diglycidyl ether of bisphenol A (Sigma–Aldrich) was used as the silica-surface modifier to prevent agglomeration. Imidazole (Sigma–Aldrich) served as the reaction catalyst.

2.2. Surface modification of silica

The silica and diglycidyl ether of bisphenol A (the modifying agent) were mixed in proportions of 40:100 wt.% and dispersed in 50 mL of toluene in the presence of imidazole (25 wt.%). The mixture was then refluxed at 100 °C for 2 h. To remove the by-product (imidazole) a centrifuging technique was used three times, with acetone as the solvent. The remaining silica was then dispersed in acetone and stirred at room temperature for 2–3 h. Finally, the acetone was removed and the silica was dried in an oven at 110 °C for a few hours.

2.3. Composite preparation

The epoxy-based composites were prepared by blending with 0.5 vol% of 130-nm and 30-nm surface-modified SiO_2particles. The silica particles were initially dispersed in the epoxy resin using ultrasonification for 20–30 min at approximately 40 °C. After adding the hardener during the next step, the mixture was manually stirred and then degassed under vacuum for 10–15 min. Finally, the mixture was poured into a closed vertical mold made of aluminum with an inner-cavity thickness of 3 mm. It needs to be pointed out that sample preparation in an ordinary horizontal mold was not successful, as we could not get rid of the air bubbles, in spite of a degassing process before pouring the mixture into the mold and additional degassing of the mixture for a few minutes when it was already in the mold. The vertical mold also reduced the time of sample preparation as only one degassing step before pouring the mixture into the mold was enough to prepare perfect, bubble-free samples. The curing was then performed in two steps. The composites were first pre-cured at 70 °C for 1 h and then post-cured at 150 °C for another hour. For comparison, neat epoxy without silica fillers was also prepared and cured in the same process as the composites.

2.4. Scanning electron microscopy (SEM)

SEM analysis using a FE-SEM Zeiss SUPRA 35VP was employed to investigate the interfacial properties in the epoxy-composite matrix on the fracture surfaces.

2.5. Raman spectroscopy

AnIn Via Reflex Raman microscope (RENISHAW) was used to collect the Raman spectra from the fracture surface of the samples. A Nikon 20× (NA = 0.90) objective was employed for all the measurements. A NdYag laser (wavelength of 532 nm) was used for the excitation. The Raman spectra were recorded with an integration time of 100 m.

2.6. Three-point bending (3PB)

The flexural properties resulting in the modulus-of-elasticity values for the neat epoxy and the silica-reinforced epoxy were determined according to the ASTM D790M-84 standard and measured on an Instron 5985 testing machine. The specimens were 60 mm long, 10 mm wide and 3 mm thick. All the experiments were performed at room temperature with a constant load rate of 1 mm min^{-1}.

2.7. Fracture toughness

Single edge-notched bending tests were performed according to the ASTM D5045-99 standard to measure the mode-I fracture toughness of the neat epoxy and the composites in terms of the critical stress-intensity factor, K_{IC}. The specimens were 44.2 mm long, 10 mm wide and 3 mm thick, with a specially designed 5 mm crack length (3-mm pre-notch plus 2-mm V-notch). The pre-notch was machine sawed and a V-notch was cut with a razor blade. All the experiments were performed at room temperature using a universal testing machine (Instron 5985) with a constant cross-head speed of 1 mm min^{-1}.

2.8. Charpy impact strength

The impact tests were performed at room temperature on specimens that were 60 mm long, 10 mm wide and 3 mm thick using a Zwick 053650 testing machine with a 1-J impactor to estimate the resistance to failure of the composite and the neat epoxy in terms of impact energy.

3. Results and discussion

3.1. Fracture-surface properties

Prior to the SEM imaging the samples were frozen in liquid nitrogen and broken by hand in order to observe the natural crack propagation in the composite. The fracture surfaces of the neat epoxy and the 30-nm and 130-nm silica/epoxy composites are shown in Fig. 1.

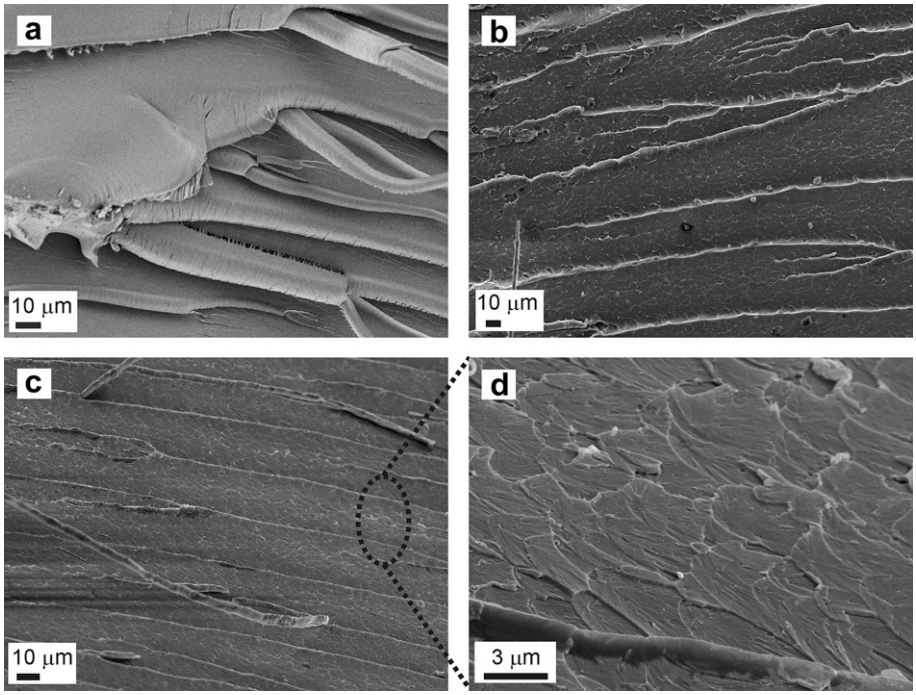

Fig. 1. Hand broken fracture surfaces of pure epoxy (a), composite with 0.5 vol% 30-nm silica fillers (b), composite with 0.5 vol% 130-nm silica fillers (c) and fracture surface detail—fish-skin-like microstructure—in 130-nm silica/epoxy composite (d).

The inclusion of silica fillers in the epoxy matrix is confirmed by the increased roughness of the composite's fracture surface compared to the smooth surface of the pure epoxy. Both silica/epoxy composites break in sharp fracture lines and characteristic steps decorated with a fish-skin-like microstructure (Fig. 1d) which in addition indicates increased brittleness compared to pure epoxy. The roughness of the fracture surface, however, slightly decreased with decreasing particle size.

It is interesting to note that individual particles did not appear to be exposed on any surface of the composite. Therefore, from the SEM images it is difficult to find out whether the cracks propagated in the matrix, through the particles or along the interface between the particles and the polymer matrix. The fracture surfaces were then additionally analyzed with Raman spectroscopy in order to obtain more information about the crack-propagation path. The fracture surfaces of each specimen, pure epoxy, 30-nm and 130-nm silica/epoxy composites and 130-nm silica particles were analyzed ten times on various spots on the fracture surface. Typical Raman spectra of the samples are shown in Fig. 2. The spectrums of epoxy and silica are characterized by characteristic peaks for the epoxide ring and the Si—O—Si bond, respectively [27]. In the spectra of both composites, however, we only found peaks characteristic for epoxy without a silica contribution. This brought us to the conclusion that the silica particles were not exposed on the fractured surface, as already observed with the SEM imaging, and that the cracks in the composites propagated in the matrix resin, so avoiding the particles.

3.2. Mechanical properties

3.2.1. Three-point bending test

The three-point bending test was used to determine the modulus of elasticity for the silica composites and the neat epoxy. Fig. 3shows a typical stress—strain curve for the samples under investigation, and in Table 1 are the corresponding elastic modulus (E) and tensile strength (UTS) values of the material. We observed an approximately 10—20% increase in E and UTS for both composites compared to the pure epoxy. The experimental scattering of both the Young's modulus and the UTS was less than 10%.

We however did not find any dramatic effect of the particle size influencing the basic material's characteristics. The 130-nm silica/epoxy composite appears to be slightly more stiff, reaching a higher overall tensile strength, compared to the 30-nm silica/epoxy composite. This is in agreement with previous studies on epoxy composites, revealing that in composites with a low volume fraction of particles the volume fraction change affects composite's mechanical properties, whereas in composites with high volume fraction of particles, the particle size plays a crucial role [25].

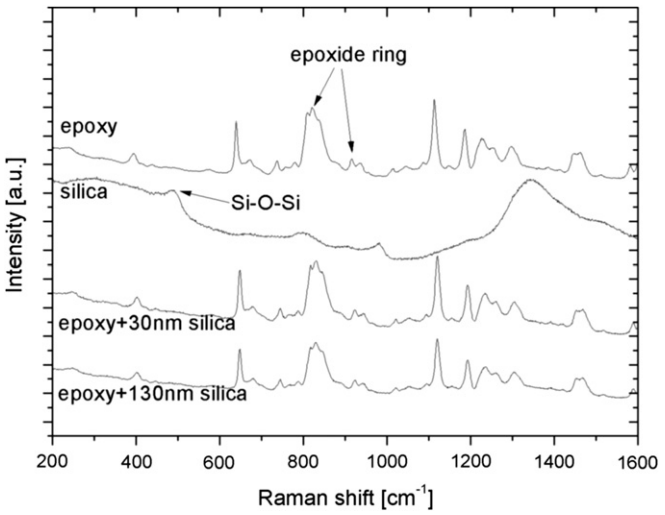

Fig. 2. Raman spectroscopy of fracture surfaces of pure epoxy, 30-nm and 130-nm silica/epoxy composites and of 130-nm silica particles.

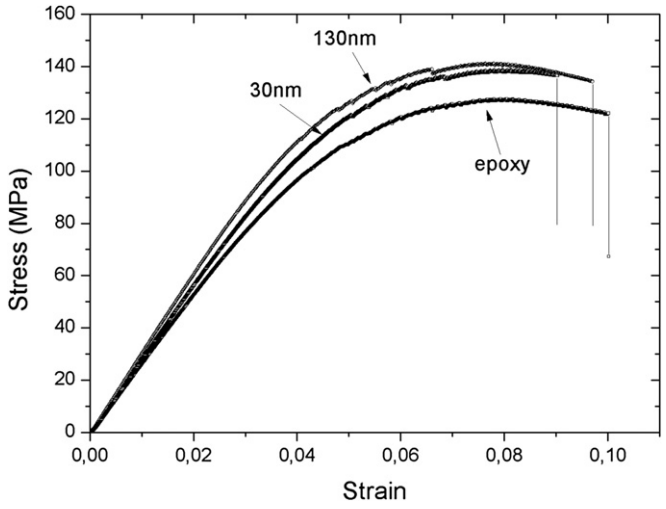

Fig. 3. Stress–strain curves of composites and neat epoxy.

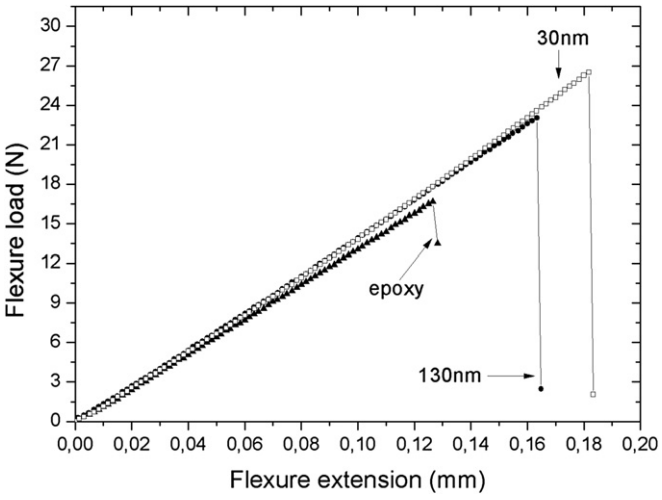

Fig. 4. Load–deflection curves of composites and neat epoxy.

Incorporation of silica fillers, on the other hand, caused the decrease in elongation at break which implies the increase of the composite brittleness and is further reflected in fracture toughness and impact strength experiments. Compared to neat epoxy, elongation at break in 130 nm and 30 nm silica/epoxy composites is reduced approximately for 5% and 10% respectively. This result is in agreement with the inversely proportional relationship of brittleness (B) to tensile elongation (ε) and storage modulus (E') as proposed by Brostow et al. [28], $B = 1/\varepsilon E'$. In the relation, use of the storage modulus accounts for the viscoelastic nature of polymers as brittle behavior arises from the solid-like rather than liquid-like behavior.

3.2.2. Fracture Toughness

The load–deflection curves of all the composites and the neat epoxy for the fracture-toughness tests are shown in Fig. 4. All the specimens showed a linear response until the brittle fracture occurred. The fracture toughness, K_{IC}, was then calculated by using linear elastic fracture mechanics [29]:

$$K_{IC} = \frac{SP_c}{BW^{3/2}} f(\xi)$$

where,

$$f(\xi) = \frac{3\xi^{1/2}\{1.99 - \xi(1-\xi)(2.15 - 3.93\xi + 2.7\xi^2)}{2(1+2\xi)(1-\xi)^{3/2}},$$

$$\xi = \frac{a_0}{W}.$$

S and P_c are the span length and the maximum load; B, W and a_0 are the thickness, the width and the pre-crack length of the specimen.

The experimental results for the fracture toughness, K_{IC}, values for the composites and the neat epoxy are listed in Table 2. The fracture toughness increased by 25–30% with the addition of silica fillers. The particle diameter, however, again had little influence on the fracture toughness in spite of change in fracture behavior and fracture surface characteristics (Fig. 1). In numbers, the composite with 30-nm silica fillers had, on average, a few percent higher fracture toughness compared to the composite with 130-nm silica fillers.

Table 2
Fracture toughness of specimens.

Sample	K_{IC} [MPa m$^{1/2}$]
Epoxy	0.66 ± 0.05
Epoxy + 0.5 vol% 130 nm SiO_2	0.91 ± 0.06
Epoxy + 0.5 vol% 30 nm SiO_2	0.93 ± 0.06

3.2.3. Charpy impact strength test

The Charpy test was used to evaluate the impact toughness of the composites and the neat epoxy. Table 3 presents the impact energy and the impact resistance for all the samples, indicating an increased impact resistance with the addition of the silica particles. Surprisingly, the results of the Charpy impact test are also clearly strongly influenced by the particle diameter. We observed an approximately 30% and 60% increase in the impact energy for the 130-nm and 30-nm silica/epoxy composites, compared to the pure epoxy.

The composite impact strength was most probably increased at the cost of reduced ductility together with formation and growth of microcracks that allow increased energy absorption. In order to understand this significant particle size dependence on impact resistance we used SEM to analyze the top surface of the broken samples close to the area, where the impactor hit the sample (Fig. 5). As shown in Fig. 5, in all three samples (a), (b) and (c) we observe material gathering in the direction of the crack propagation caused by the impact and characteristic steps with increased roughness in both composites that indicate the nature of brittle

Table 1
Elastic modulus (E), tensile strength (UTS) and elongation at break of specimens.

Sample	E [GPa]	UTS [MPa]	Elongation at break [%]
Epoxy	2.6	127	10.0
Epoxy + 0.5 vol% 130 nm SiO_2	3.0	141	9.6
Epoxy + 0.5 vol% 30 nm SiO_2	2.8	138	9.0

Table 3
Impact energy and impact resistance of the specimens.

Sample	Impact energy [J]	Impact resistance [kJ m^{-2}]
Epoxy	0.19 ± 0.02	6.4 ± 0.7
Epoxy + 0.5 vol% 130 nm SiO_2	0.26 ± 0.02	8.9 ± 0.6
Epoxy + 0.5 vol% 30 nm SiO_2	0.33 ± 0.03	10.8 ± 0.7

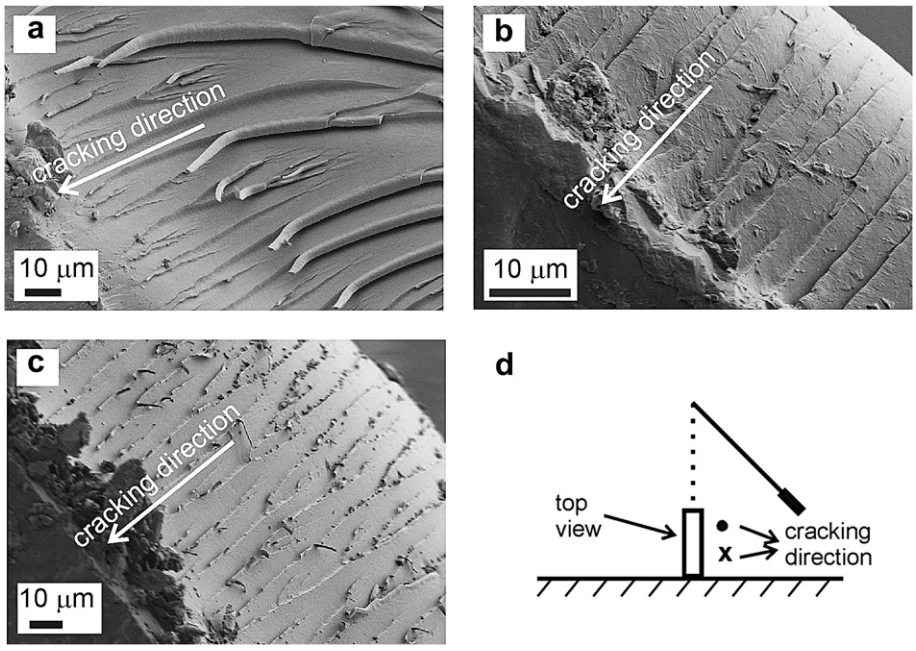

Fig. 5. SEM images of the top view of the broken samples of pure epoxy (a), composite with 0.5 vol% 30-nm silica fillers (b), composite with 0.5 vol% 130-nm silica fillers (c) after the Charpy impact strength test and experimental geometry of Charpy impact strength test (d). SEM images were taken close to the area where the impactor hit the sample.

behavior [30]. As already shown in Fig. 1, where the samples were broken by hand, the details of the damaged surface close to the area where the impactor hit the sample differ for pure epoxy and both composites also in Charpy impact-strength test. In pure epoxy (Fig. 5a) the surface remains smooth with smooth steps and slight matrix delamination. In 30 nm and 130 nm silica/epoxy samples (Fig. 5b, c)we however observed increased roughness and sharp steps compared to pure epoxy sample with excess pieces of the material and more pronounced delamination which additionally increases the energy absorption capability of the material.

4. Conclusion

We investigated the mechanical properties of epoxy composites filled with a low, 0.5% volume fraction of 130-nm and 30-nm spherical silica particles. SEM observations revealed the impact of the silica fillers on the epoxy matrix through an increased roughness of the fracture surface compared to the smooth neat-epoxy surface. We observed the appearance of characteristic steps decorated with a fish-skin-like microstructure on the composite fracture surface indicating increased brittleness compared to pure epoxy. The Raman spectroscopy indicated, together with the SEM observations, that the cracks in the composites filled with a low volume fraction of silica particles propagated in the matrix resin, thereby avoiding the particles.

We have shown that in spite of low volume fraction of silica particles in epoxy matrix, the mechanical properties are significantly improved. The results of the three-point bending test showed a 10–20% increased stiffness in both composites as well as an increased tensile strength (UTS) compared to the pure epoxy. On the contrary, elongation at break decreased for 5–10% in both composites compared to neat epoxy, confirming brittle fracture behavior in composites. The fracture toughness results showed a 25–30% improvement in the toughness for both composites, compared to the pure epoxy. The Young's modulus and the mode-I fracture toughness of the composites showed no characteristic dependence on the particle diameter. However, the composites' resistance to failure in terms of impact energy was, on the other hand, strongly dependent on the silica size: we observed a 30% increase for the 130-nm, and 60% increase for 30-nm, silica/epoxy composites, compared to the pure epoxy.

Acknowledgments

The authors gratefully acknowledge The Research Foundation–Flanders (FWO) for the financial support enabling research work at K. U. Leuven. This work was partly carried out within the framework of the Slovenian programme P2-0132, "Fizika in kemija površin kovinskih materialov" of the Slovenian Research Agency, whose support is gratefully acknowledged by M. Conradi and A. Kocijan.

References

[1] S.Q. Deng, L. Ye, K. Friedrich, J. Mater. Sci. 42 (2007) 2766–2774.
[2] L.E. Nielsen, R.F. Landel, Mechanical Properties of Polymers and Composites, Marcel Dekker, New York, 1994.
[3] Z. Hashin, J. Appl. Mech. Trans. Asme 50 (1983) 481–505.
[4] R.W. Rice, Mechanical Properties of Ceramics and Composites, Marcel Dekker, New York, 2000.
[5] A.C. Moloney, H.H. Kausch, T. Kaiser, H.R. Beer, J. Mater. Sci. 22 (1987) 381–393.
[6] J. Spanoudakis, R.J. Young, J. Mater. Sci. 19 (1984) 487–496.
[7] M. Hussain, Y. Oku, A. Nakahira, K. Niihara, Mater. Lett. 26 (1996) 177–184.
[8] E.P. Giannelis, Appl. Org. Chem. 12 (1998) 675–680.
[9] T. Lan, T.J. Pinnavaia, Chem. Mat 6 (1994) 2216–2219.
[10] A.S. Zerda, A.J. Lesser, J. Polym. Sci. Part. B-polym. Phys. 39 (2001) 1137–1146.
[11] R.P. Singh, M. Zhang, D. Chan, J. Mater. Sci. 37 (2002) 781–788.
[12] R.A. Pearson, A.F. Yee, J. Mater. Sci. 26 (1991) 3828–3844.
[13] C.B. Bucknall, G. Maistros, C.M. Gomez, I.K. Partridge, Makromol. Chem., Macromol. Symp. 70-1 (1993) 255–264.
[14] R.A. Pearson, A.F. Yee, Polymer 34 (1993) 3658–3670.
[15] M. Frounchi, T.A. Westgate, R.P. Chaplin, R.P. Burford, Polymer 35 (1994) 5041–5045.
[16] F. Stricker, Y. Thomann, R. Mulhaupt, J. Appl. Polym. Sci. 68 (1998) 1891–1901.
[17] R.T. Quazi, S.N. Bhattacharya, E. Kosior, J. Mater. Sci. 34 (1999) 607–614.
[18] T. Adachi, W. Araki, T. Nakahara, A. Yamaji, M. Gamou, J. Appl. Polym. Sci. 86 (2002) 2261–2265.
[19] A. Boonyapookana, K. Nagata, Y. Mutoh, Compos. Sci. Technol. 71 (2011) 1124–1131.
[20] S.V. Kamat, J.P. Hirth, R. Mehrabian, Acta Metall. 37 (1989) 2395–2402.
[21] F.F. Lange, K.C. Radford, J. Mater. Sci. 6 (1971) 1197–1203.

[22] A.F. Bower, M. Ortiz, J. Appl. Mech. Trans. Asme 60 (1993) 175–182.
[23] A.G. Evans, Philos. Mag. 26 (1972) 1327–1344.
[24] A. Moisala, Q. Li, I.A. Kinloch, A.H. Windle, Compos. Sci. Technol. 66 (2006) 1285–1288.
[25] S.C. Kwon, T. Adachi, W. Araki, Compos. Part B-Eng. 39 (2008) 773–781.
[26] M. Zorko, S. Novak, M. Gaberscek, J. Ceram. Process Res. 12 (2011) 654–659.
[27] L. Huber, B.V. Jose, Marcel Dekker, New York, 2003.
[28] W. Brostow, H.E.H. Lobland, J. Mater. Sci. 45 (2010) 242–250.
[29] W.T. Koiter, J.P. Bentham, Asymptotic Approximation to Crack Problems, , In: Methods of Analysis and Solutions of Crack Problems, Leyden, Nordhoff, 1973.
[30] J.W. Johnson, D.G. Holloway, Philos. Mag. 14 (1996) 731–743.